INTERNATIONAL JOURNAL OF AGRICULTURE & BIOLOGY
ISSN Print: 1560–8530; ISSN Online: 1814–9596
18–0426/2018/20–9–1970–1978
DOI: 10.17957/IJAB/15.0716
http://www.fspublishers.org

Full Length Article

Evaluation of Spectral Disease Index PMI to Detect Early Wheat Powdery Mildew using Hyperspectral Imagery Data

Fenfang Lin[1], Dandan Wang[1], Dongyan Zhang[2*], Xiaodong Yang[3*], Xun Yin[2] and Daoyong Wang[2]
[1]*School of Geography and Remote Sensing, Nanjing University of Information Science & Technology, Nanjing 210044, China*
[2]*Anhui Engineering Laboratory of Agro-Ecological Big Data, Anhui University, Hefei 230601, China*
[3]*Key Laboratory of Quantitative Remote Sensing in Agriculture of Ministry of Agriculture, Beijing Research Center for Information Technology in Agriculture, Beijing100097, China*
[*]For correspondence: zhangdy@ahu.edu.cn; yangxd@nercita.org.cn
[*]Equal contributors

Abstract

Powdery mildew is one of the most widely destructive plant diseases, particularly infecting winter wheat. Early detection of wheat powdery mildew is of importance, which is useful to reduce economic costs and environmental pollution. However, difficulties emerge at early development stages, due to slight variations of the characteristic symptoms. Fortunately, hyperspectral reflectance imaging has been proven as a powerful tool to detecting early disease severity in plant. In this study, hyperspectral imagery data of leaves were acquired at early stages of the disease in winter wheat. It was demonstrated that early powdery mildew could induce observable spectral changes in both visible and near infrared regions. Given that, powdery mildew indices (PMI) were constructed and showed the capability of distinguishing between normal and diseased leaves, although it displayed poor effects for differentiating disease-damaged levels of early powdery mildew and estimating disease severity. However, further study was carried out by combination of hyperspectral vegetation indices closely related to plant diseases. It was noticeable that the model of three indices of PRI, PSRI and ARI significantly increased the classification accuracy of various early disease levels, and the regression model of PMI, PSRI and ARI apparently improved the estimation accuracy of disease severity. These valuable results could be used to prevent the development and the spread of the disease, and particularly beneficial to develop a portable or automated sensor in precision agriculture.

Keywords: Wheat powdery mildew; Hyperspectral imaging; Spectral disease index; Early detection

Introduction

Wheat powdery mildew is one of the major diseases affecting the worldwide wheat production nowadays, which reduces the plant photosynthetic ability, lowers productivity and poor grain quality (Zhang *et al.*, 2012; Ray *et al.*, 2017). The detection and differentiation of powdery mildew at early stages not only allow timely treatment, resulting in limited yield loss and reducing fungicides usage, but also offer an optimal timing for fungicide application and avoid the build-up of resistance (Sankaran *et al.*, 2010; Jafari *et al.*, 2016). Therefore, it is important to identify and quantify early stress responses before irreversible damages occur. The disease mainly affects leaves of wheat. The characteristic symptoms at early development stages are the initial formation of scattered white filamentous mildew on the leaf surface, probably 1–2 mm white mildew. These unobvious variations are challenge to early detection of the powdery mildew.

The traditional detecting way of the disease is expensive and inefficient. Due to shorter time from early warning to prevention and treatment, the method could directly delay the best disease prevention opportunity. However, remote sensing technology is a powerful tool for effectively detecting and diagnosing powdery mildew, due to its advantages including fast, real-time and non-destructive monitor (Mahlein *et al.*, 2012a, b; Yuan *et al.*, 2014; De Castro *et al.*, 2015; Martinelli *et al.*, 2015). Zhang *et al.* (2012) analyzed spectral changes and extracted various spectral features of infected leaves by vegetation indices and the continuous wavelet method. Huang *et al.* (2013) also compared sensitive wavebands of the first, second and third leaf in the whole wheat plant using correlation coefficient and continuous wavelet transform methods in detail. Cao *et al.* (2013) demonstrated that canopy hyperspectral reflectance can be an efficient way for wheat powdery mildew detection without other stresses resulting in unhealthy symptoms. To rapidly and precisely

To cite this paper: Lin, F., D. Wang, D. Zhang, X. Yang, X. Yin and D. Wang, 2018. Evaluation of spectral disease index PMI to detect early wheat powdery mildew using hyperspectral imagery data. *Int. J. Agric. Biol*., 20: 1970–1978

distinguish powdery mildew from other diseases, Huang *et al.* (2014) constructed a powdery mildew index (PMI) based on hyperspectral data measured with a spectroradiometer, which had the classification accuracy of 86.5% for healthy leaves and leaves infected with powdery mildew and good correlation with the disease index. These studies mainly used visible and infrared spectroscopy for detecting powdery mildew in wheat after medium-term developing stages of the disease. Symptoms of the disease are obvious and highly visible at later stages, which can result in spectral changes in visible/NIR ranges captured by hyperspectral spectrometers. Non-imaging hyperspectral sensors measure the spectral reflectance at a single circular measurement spot, which always represents the mean of the reflectance of healthy and diseased plant tissue (de Jong *et al.*, 2012). If varying surface characteristics exist in the spot, the physically averaged reflectance contains diseased and non-diseased information. This indicates that minor changes in leaf reflectance will be weakened by averaging way at early infection stages (Behmann *et al.*, 2014). A precise classification is very complicated at early stages or in the case that only few pustules occur. This is due to the fungal tissue on the leaf surface shifting the spectral signature like a dusty coat (Rumpf *et al.*, 2010). However, imaging sensor systems consist of pixels, which make it easy to identify a pixel wise attribution of disease specific symptoms and tissue (Steiner *et al.*, 2008; Rumpf *et al.*, 2010). Chaerle and van der Straeten (2000) reported that imaging hyperspectral sensors can improve hyperspectral disease detection through a better understanding of the pathogen host interactions. Previous studies also indicated that hyperspectral imaging techniques could be more robust in disease detection in plant diseases than spectroscopic methods alone, particularly at early infection stages (Del Fiore *et al.*, 2010; Sankaran *et al.*, 2010; Behmann *et al.*, 2014; Jafari *et al.*, 2016).

Therefore, this study focused on detection of wheat powdery mildew at early stages. The main objectives of this study were to: (1) examine spectral response of the early disease in visible and NIR ranges based on imaging data, (2) construct PMIs for early powdery mildew and investigate its sensitivity to the early disease (3) combine PMIs with several hyperspectral vegetation indices closely related to diseases for detective ability of early powdery mildew and evaluate them.

Materials and Methods

Study Site and Leaf Sampling

The experimental field located at Beijing Academy of Agriculture and Forestry Science, China (39°56'N, 116°16'E). The cultivar of winter wheat was 'jingshuang 16', which was widely grown and is highly susceptible to powdery mildew. Wheat powdery mildew can occur on different growth stages, however, the disease at lately booting stage spread rapidly under appropriate natural environment, so that this growth stage was regarded as early infected moment of wheat powdery mildew in this study. Meanwhile, to provide important support to conduct preventive procedure such as fungicide spray, we performed the experiments at the period of filling stage.

Leaf samples were collected in the field and rapidly transported to a nearby indoor laboratory for imaging spectrometer data measurements. In this process, a water loss and cross contamination in leaves was reduced to the minimum as much as possible. The detail method was found in Zhang *et al.* (2012). A total of 70 leaf samples were collected for measurement, including 28 normal leaves and 42 diseased leaves with different slight severity.

Hyperspectral Imaging Systems

Imaging spectrometer data of leaves were acquired by the customized visible and near-infrared hyperspectral imaging system. The components of the system have been showed in Fig. 1. The spectral range of the system is between 400–1000 nm. The sampling interval of the spectrum is about 0.8 nm and the spectral resolution is 2.8 nm. The CCD camera has high sensitivity in the visible/near infrared region and a wide dynamic range of 12-bit digital output. The illumination consisted of two halogen lamps fixed by the angle of 45° and adjustable height to make sure leaves under uniform and even light. The object distance and the exposure time were respectively set at 410 mm and 90 ms during measurement process to prevent images from being blurred or deformed (Yang *et al.*, 2015).

Image Acquisition and Calibration

Imaging spectrometer data of winter wheat leaves was collected by the above hyperspectral imaging system. The samples passed its view slot by the electric moving stage when the CCD camera was fixed over the stage. In this process, there were appropriate intensity of illumination and exposure time of the camera. Then, the images were acquired line-by-line.

Due to the different spectral response of the spectrometer in the VIS/NIR region, there was the influence of the internal dark current when the operating temperature is too low/high. This resulted in large image noises in the wavebands with weak spectral response. Therefore, spectral calibration was performed for the dark current correction to eliminate parts of the data noises using the following formula:

$$I = \frac{I_0 - B}{W - B} \quad (1)$$

Where, I and Io are the relative and original reflectance intensity of each wavelength, respectively, B is the intensity of the dark current, W is the reflectance intensity of the standard white board.

Appendix

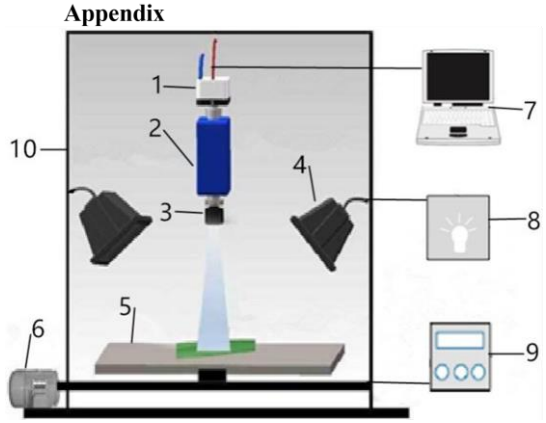

Fig. 1: The hyperspectral imaging system is consisted of: (1) CCD camera; (2) imaging spectrograph; (3) lens; (4) light source; (5) sample stage; (6) electric moving stage; (7) computer; (8) light source controller; (9) moving stage controller; (10) dark room

Data Preprocessing

The normalized reflectance was computed to suppress environmental noises (Pu *et al.*, 2008). A band reflectance was replaced with the following formula:

$$\rho_i^{'} = \rho_i \Big/ \left(\frac{\sum_{i=1}^{N} \rho_i}{N}\right) \quad (2)$$

Where, $\rho_i^{'}$ is the normalization value, ρ_i is the original reflectance, and N is the number of waveband.

Determination of Disease Index

The disease index (DI) was used to describe the infected severity of powdery mildew. The DI of each leaf sample was determined by two processes. Firstly, the severity of wheat powdery mildew was estimated by computer calculation and visual judgment of a percentage of an infected leaf surface area on the blade. Secondly, the estimated severity was divided into 4 categories to minimize human error for obtaining the disease index (DI), referring to Chinese Standard (NY/T 613-2002):0–3% (no disease), 3–10% (DI=1), 10.1–20% (DI=2), 20.1–30% (DI=3). DI was taken as a continuous variable in subsequent regression analysis. In addition, two discrete levels for the disease severity of leaves were used for subsequent discrimination analysis. These categories are very slight disease (the lesion percentage ranging from 5% to 15%) and slight disease (the lesion percentage ranging from 15% to 30%).

Analytical Methods

The construction of PMI based on the RELIEF-F algorithm: Spectral indices can effectively identify specific plant diseases (Mahlein *et al.*, 2013). In this study, the powdery – mildew index (PMI) was constructed by the RELIEF-F algorithm proposed by Huang *et al.* (2014).

The RELIEF-F algorithm was designed to measure how well attributes distinguished between instances within the close proximity of each other (Kira and Rendell, 1992; Robnik-Sikonja and Kononenko, 2003). Therefore, the algorithm was useful in finding some wavelengths for specific diseases. It can deal with more than two class problems, particularly incomplete and noisy data. Its ability to select features depends on the number of nearest neighbors (k). For a fixed k, the set of k nearest neighbors of the same class or a different class were deemed a "hit" or a "miss" (Kira and Rendell, 1992; Mahlein *et al.*, 2013). According to attributes of response vector, the RELIEF algorithm can be used for classification or regression analysis.

PMI consisted of a relevant single wavelength and a normalized wavelength difference. It was shown as the following formula:

$$PMI = \frac{R_1 - R_2}{R_1 + R_2} \pm 0.5R_3 \quad (3)$$

Where, R_1 and R_2 are reflectance in normalized wavelengths, R_3 is reflectance in the most relevant single wavelength.

The most relevant single wavelength and normalized wavelengths were obtained by the RELIEF-F algorithm. According to Huang *et al.* (2014), the most sensitive single wavelength was among wavelengths of the highest weighted (20%). Two normalized wavelengths were wavelengths from the best and worst weighted wavelengths (10%), respectively. And the distance between the two wavelengths was less than 50 nm.

Other Hyperspectral Vegetation Indices Compared to PMI

To conduct a thorough comparison with PMI in disease detection, a total of 11 hyperspectral vegetation indices were included and examined (Table 1). These hyperspectral indices have been evaluated to be useful for disease detection or have a potential in detecting stress (Mahlein *et al.*, 2013).

Discrimination Analysis of Disease Severity by Spectral Indices

Discriminant models for differentiating disease levels were constructed using Fisher linear discriminate analysis (FLDA) based on PMI and selected spectral indices with high sensitivity to disease severity, separately. To examine the sensitivity of these spectral indices in detecting the powdery mildew, Wilks' lambda was applied to select optimal spectral indices when PMI and other hyperspectral indices were independents.

Table 1: Commonly used hyperspectral vegetation indices for plant disease detection

Indices	Definition	Description or formula	Literatures
NBNDVI	Narrow-band normalised difference vegetation index	(R850 - R680)/ (R850 + R680)	Thenkabail *et al.* (2000)
NRI	Nitrogen reflectance index	(R570 - R670)/ (R570 + R670)	Filella *et al.* (1995)
TVI	Triangular vegetation index	0.5[120(R750-R550)-200(R670 - R550)]	Broge and Leblanc (2001)
PRI	Photochemical/Physiological Reflectance Index	(R531 - R570)/ (R531 + R570)	Gamon *et al.* (1992)
PhRI	The Physiological Reflectance Index	(R550 - R531)/ (R550 + R531)	Gamon *et al.* (1992)
CARI	Chlorophyll absorption ratio index	(| (a670 + R670 + b) |/ (a2 + 1)1/2) - (R700/R670) a = (R700 - R550)/150, b = R550 - (a - 550)	Kim *et al.* (1994)
TCARI	The transformed chlorophyll absorption and reflectance index	3[(R700 - R670) - 0.2(R700 - R550) (R700/R670)]	Haboudane *et al.* (2004)
MCARI	Modified chlorophyll absorption ratio index	[(R701 - R671) - 0.2(R701 - R549)]/(R701/R671)	Daughtry *et al.* (2000)
RVSI	Red-Edge Vegetation Stress Index	[(R712 + R752)/2] - R732	Merton and Huntington (1999)
PSRI	Plant Senescence Reflectance Index	(R680 - R500)/R750	Merzlyak *et al.* (1999)
ARI	Anthocyanin Reflectance Index	$(R550)^{-1}$ - $(R700)^{-1}$	Gitelson *et al.*(2001)

The criterion of variables for entry or removal is probability of F value. Finally, four statistics were selected to evaluate the discriminant model: overall accuracy (OAA), producer's accuracy, user's accuracy, and kappa coefficient.

Estimation of Disease Severity by Spectral Indices

In addition to the discrimination among different disease levels, two regression models were constructed for estimating DI, One of which was based on PMI while the other one was based on optimal spectral features. To establish the regressive model between DI and optimal spectral features, multiple stepwise regression analysis was applied for estimating DI. This algorithm first uses the stepwise method to determine how many independent variables are entered into the analysis by probability of F value. Finally, the multivariate model was constructed according to selected spectral indices. The coefficient of determination (R^2) and the relative root mean square error (RMSE) were used for evaluating the performance of models. In this study, FLDA analysis and multiple stepwise regression analysis were implemented in SPSS 20.0.

Results

Leaf Spectral Characteristics of Winter Wheat under Early Powdery Mildew Stress

Based on three different severity classes on early powdery mildew specified as described, Fig. 2 shows curves of normalized spectra and first-derivative spectra. The shapes of spectral curves of normal and diseased leaves for normalized spectra and derivative spectra were similar, but several differences existed in specific wavelength ranges among the three disease severity categories (Fig. 2a and b). At 450−700 nm, the reflectance value of normal leaf in red edge region had minimal value, followed by very slight and slight leaves had the highest value. At 750−1000 nm, normal leaves had highest reflectance value, followed by very slight leaves and slight leaves had lowest reflectance value. The more serious the disease was, the higher reflectance of leaves was in the visible region, but the result was the opposite in the near-infrared region.

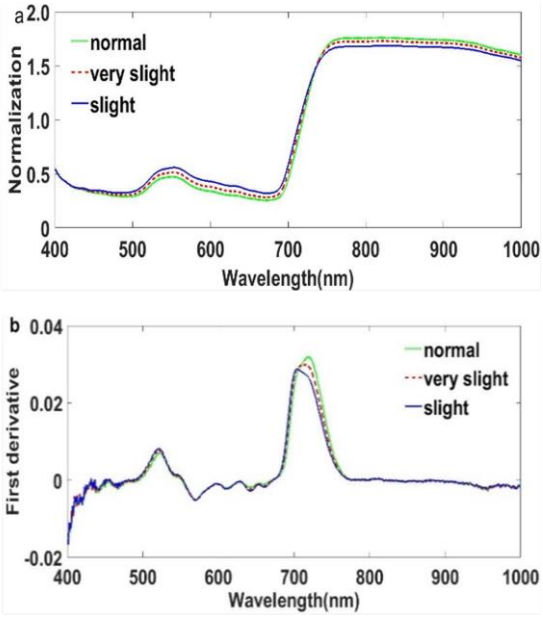

Fig. 2: Curves of normalized spectra, first derivative spectra and normalized reflectance ratios of diseased leaf spectra to normal spectrum. (a) Normalized reflectance curves of normal, very slightly-damaged (3% < lesion portion < 15%) and slightly-damaged leaves (15% lesion portion 30%); (b) first derivative spectral curves of normal and diseased leaves

These results were consistent with previous studies in metaphase of powdery mildew (Zhang *et al.*, 2012; Huang *et al.*, 2013). However, Fig. 2b showed that differences of the first derivative spectra between normal and diseased leaves were significant in the red edge region from 690 to 740 nm, but not obvious in the green edge region from 510 to 530 nm. This may be related to minor damages in plants at early developing stages of the disease.

Detection of Early Powdery Mildew Stress by the Powdery Mildew Index (PMI)

Discrimination analysis with PMI: The RELIEF-F algorithm was one of feature selection algorithms,

which determined importance of attributes by computing ranks and weights of attributes for classification and regression. Fig. 3 illustrates single wavelength weights for discrimination analysis with two severity classes and three severity classes. These two weight curves had similar shape and basically identical waveband position for some peaks/valleys, only differed in weight values. This was attributed to small difference between diseased levels at early stage of powdery mildew. As shown in Fig. 3, single wavelengths around 690, 820, and 910 nm had high relevance to diseased winter wheat leaves, and the normalized reflectance differences were around 445 and 680 nm. All possible wavelength combinations were calculated for the specific spectral index by the RELIEF-F algorithm. Finally, the most relevant single wavelengths for two disease levels and three disease levels were 836 nm and 685 nm, respectively. But the wavelengths for computing normalized wavelength difference were same, including 687 nm and 446 nm. Two powdery – mildew indices were proposed based on above wavelengths (Table 1).

For evaluating the ability of PMI for differentiating disease levels, the discriminant analysis models for these two systems of severity classification were established. The classification results with cross validation approach were listed in Table 2a, b. The classification accuracy and the Kappa indices of PMI for the two health levels were 0.89 and 0.77, respectively. In addition, it is noticeable that producer's and user's accuracies for the PM-infected class were both more than 80%. These results were in agreement with Huang *et al.* (2013). However, the model for distinguishing three healthy levels can also yield an acceptable accuracy, although its classification accuracy is not as high as that for the two health levels. But smaller producer's and user's accuracies were achieved for the very slightly-damaged class and the slightly-damaged class with the discriminant model for the three health levels compared to the other levels. These results showed that the PMI were able to distinguish between healthy and PM-infected leaves with good reliability, although discriminant accuracies for the very slightly-damaged level and the slightly-damaged level may be further increased by addition of other spectral features in the model.

Regression Analysis with PMI

Other than determining the disease severity levels of leaves by discrimination analysis, we also attempted to estimate the DI value in a continuous manner by regressive models with PMI. In order to find proper wavelengths for PMI construction estimated DI, the RELIEF algorithm was performed in a way of regression analysis. The curve of single wavelength weights was shown in Fig. 3. It revealed that the shape of the curve was similar to those for classification analysis, which is due to small number of disease severity levels. However, features of peaks/valleys between curves were different.

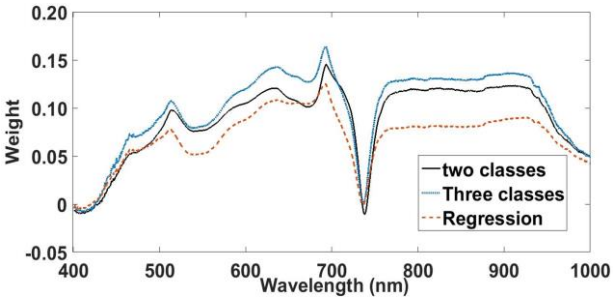

Fig. 3: Single wavelength weights for discrimination analysis with two severity classes and three severity classes and regression analysis of PMI with disease severity

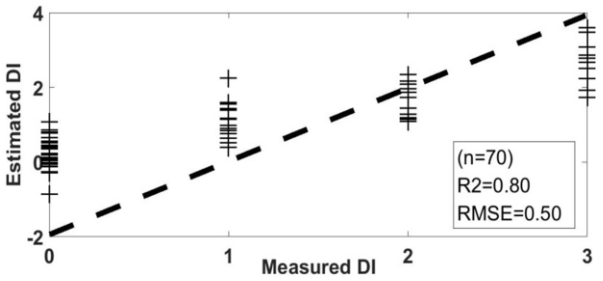

Fig. 4: Scatter plots between measured DI and estimated DI for the regression model with PMI

Finally, PMI for estimating DI was adopted based on reflectance at 913 nm and normalized reflectance difference between 443 and 686 nm. Then, statistical correlation analysis was carried out between the PMI and the DI, and the linear regression model with PMI was established (Fig. 4). It was found that the DI has significant positive correlation to the PMI (R^2=0.798, n=70). This indicated that the PMI showed potential for monitoring the early severity of powdery mildew.

Detection of Early Powdery Mildew Stress by a Combination of PMI and Hyperspectral Vegetation Indices

Discrimination analysis with optimal spectral indices: Apart from examining the ability of PMI for discriminating disease severity and estimating disease index (DI), the detective analysis of early powdery mildew stress was performed based spectral features PMI combined with other hyperspectral vegetation indices, which will show comparison among these indices. Table 2a, b showed that probability of F and Wilks' lambda of all spectral indices for two classification systems in the process of stepwise discriminant analysis, which can be interpreted as their sensitivity to the disease severity levels. It is easy to see that there were different numbers of optimal spectral features chosen as sensitive variables into discriminant models in two classification systems, according to probability of F and Wilks' lambda.

Table 2a: The classification accuracies created based on cross validation approach for discriminant models with PMI

Samples	P.′s.a (%)	U.′s.a (%)	OAA	κ	PMI formula
	Two classes				
Healthy	96.43	84.38	0.89	0.77	$\frac{R687-R446}{R687+R446}-0.5R_{836}$
Powdery mildew	83.33	92.11			
	Three classes				
Normal	92.86	86.67	0.81	0.71	$\frac{R687-R446}{R687+R446}-0.5R_{685}$
very slight	74.07	76.92			
slight	73.33	78.57			

Table 2b: Probability of F and Wilks's Lambda of all variables in stepwise discriminant analysis for 2-class system and 3-class system

Indices	Probability of F		Wilks' Lambda		Indices	Probability of F		Wilks' Lambda	
	2-class system	3-class system	2-class system	3-class system		2-class system	3-class system	2-class system	3-class system
NBNDVI	.339	.648	.350	.153	ICARI	.505	.141	.350	.146
NRI	.794	.101	.355	.144	MCARI	.395	.287	.351	.149
TVI	.434	.629	.352	.153	RVSI	.122	.310	.343	.150
PRI	.049	.006	.377	.182	PSRI	.837	.006	.355	.181
PhRI	.710	.220	.355	.148	ARI	.000	.000	.652	.285
CARI	.367	.156	.351	.146	PMI	.743	.446	.355	.151

For the two-class system, the two indices of PRI and ARI were as predictor variables into the identification model. However, for the three-class system the index PSRI was chosen to enter the discriminant mode in addition to PRI and ARI.

Meanwhile, it is apparent that PMI was not chosen as one of the best spectral features when PMI and other 11 hyperspectral vegetation indices were alternative indices for discriminant models. However, subtle differences were viewed from classification accuracies for models (Table 3). For the two-class system, the overall accuracy and the Kappa indices of the model with PRI and ARI were basically the same as those of the model with PMI, although small differences were shown in producer's and user's accuracies. This indicated that PMI can be better contributed to the development of a portable sensor for precision agriculture, compared to PRI and ARI. But for the three-class system, the overall accuracy and the Kappa indices of the model with PRI, PSRI and ARI were higher than those of the model with PMI. Obviously, this was due to the significant increase of producer's accuracies for the very slightly-damaged level and the slightly-damaged level. This implied that the combination of the three indices of PRI, PSRI and ARI had the better distinguishing capability for the very slightly-damaged level and the slightly-damaged level.

Table 3: The classification accuracies created based on cross validation approach for discriminant models with optimal spectral indices

Samples	P.′s.a (%)	U.′s.a (%)	OAA	κ	Best spectral features
			Two classes		
Healthy	92.86	81.25	0.89	0.77	PRI,ARI
Powdery mildew	85.71	94.74			
			Three classes		
Normal	92.86	89.66	0.87	0.80	PRI,PSRI,ARI
very slight	85.19	82.14			
slight	80.00	92.31			

Table 4: Summary of correlation analysis between spectral features and DI

Rank	Indices	R	R^2	Significance (p-value)
1	PMI	0.893	0.798	0.000
2	NBNDVI	-0.860	0.740	0.000
3	ARI	0.854	0.729	0.000
4	PSRI	0.835	0.697	0.000
5	TVI	-0.766	0.587	0.000
6	MCARI	0.759	0.576	0.000
7	PRI	-0.758	0.575	0.000
8	CARI	0.724	0.524	0.000
9	TCARI	0.572	0.327	0.000
10	RVSI	0.564	0.318	0.000
11	PhRI	0.216	0.047	0.073
12	NRI	-0.169	0.029	0.162

Regression Analysis with Optimal Spectral Indices

To compare the estimating ability of disease index between PMI and other hyperspectral vegetation indices, Table 4 summarized the results of correlation analysis between each of the 12 spectral features and DI of the 70 samples. It turned out that ten indices significantly correlated with DI (p-value < 0.05). Of them, four indices had an absolute R value which is over 0.8. They were PMI, NBNDVI, ARI and PSRI, of which PMI had the highest R value. This indicated that PMI had powerful sensitivity to leaf powdery mildew. In order to further determine optimal spectral indices, the stepwise method was used to select variables for the multivariate model. Table 5 displayed the related variables and their coefficients for the model. Spectral features selected were PMI, PSRI and ARI. The relative RMSE and R square were 0.41 and 0.86, respectively (Fig. 5). To some extent, the estimating accuracy for DI was improved by addition of PSRI and ARI.

Table 5: Coefficients of variables in multivariate regression model*

variables	Coefficients	T	Sig.
PMI	8.120	4.297	0.000
PSRI	52.040	3.828	0.000
ARI	3.510	3.321	0.001
Constant	9.586	5.923	0.000

*: 95% confidence interval for coefficient; t statistics and two-tailed probability of *t*

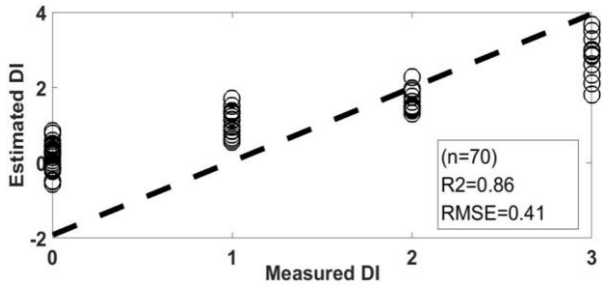

Fig. 5: Scatter plots between measured DI and estimated DI for the regression model with optimal vegetation indices

Discussion

In the hyperspectral imaging, a leaf is scanned for a set of pixels. The resulting information simultaneously includes imagery and spectrum (West *et al.*, 2003; Govender *et al.*, 2009). Therefore, we can acquire reflectance data for any region of interest in a leaf, e.g. whiting spots in leaves. In our study, Fig. 2 showed spectral responses of early powdery mildew based on leaf imaging data. Compared with spectral characteristics of powdery mildew after medium-term of the disease (Zhang *et al.*, 2012; Huang *et al.*, 2013, 2014) It was found that variation laws of reflectance with disease severity in the visible and near-infrared (NIR) regions were similar, but reflectance differences between normal and diseased leaves were not as obvious as those at the middle and late stages. Moreover, our study pointed out that the spectral reflectance in the range of 500–740 nm, responded significantly to powdery mildew, with the "blue shifting" phenomenon. These spectral changes may be due to the breakdown of chlorophyll pigments, the powder on the leaf's surface and subsequent changes of other pigments in diseased leaves as well as the breakdown of the cell structure (West *et al.*, 2003; Sankaran *et al.*, 2010; Zhang *et al.*, 2012). In addition, small spectral differences between normal and diseased leaves may result from less obvious symptoms at early stage than those after the time. Wheat leaves are mainly influenced by powdery mildew. The early symptoms are the initial formation of scattered white filamentous mildew on the leaf surface, probably 1–2 mm white mildew. Then, infected parts of leaves often turn yellow leaf and blight. With time elapsing after leaves were inoculated, the disease severity of leaves becomes explicit.

Based on spectral responses of early powdery mildew, a new hyperspectral index for detection of powdery mildew was constructed by RELIEF-F algorithm. This can be contributed to development of portable disease-detected sensors, which offers an optimal timing for fungicide application in crop management and reduce loss of crop yield. According to weights of wavelengths, a single wavelength and a normalized wavelength difference were thoroughly searched for the best weighted combination. Whether discrimination or regression analysis, normalized wavelength differences for detection of early powdery mildew were all located around 446 and 687 nm, whereas single wavelengths of high relevance were different, the former was 836 nm with two-class system and 685 nm with three-class system, the latter was 913 nm. For discrimination and regression analysis, the PMIs for detection of early powdery mildew mainly used three narrow bands in the red, blue and NIR region (i.e. 446 nm, 687 nm, 685 nm, 836 nm and 913 nm), which were associated with variations of plant pigment and the change of plant cell structures. The result was corresponding to spectral response of early powdery mildew. However, this was not consistent with that after medium-term stages of the disease, of which PMI was mainly located in the green edge and red edge (Mahlein *et al.*, 2013; Huang *et al.*, 2014). Table 1 and Fig. 4 illustrated the distinguishing and estimating ability of PMI for powdery mildew, respectively. Classification by the PMI resulted in a very good discrimination between powdery mildew and healthy wheat leaves. However, difficulties remained in the identification of very slight and slight powdery mildew infection. Other researchers also demonstrated that at disease severities below 25% the classification error was high, due to minor changes in leaf reflectance at early infection stages (Mahlein *et al.*, 2013). A significant positive correlation was found between the DI and the PMI, which was in agreement with Huang *et al* (2014). But low RMSE indicated that the combination of PMI with other hyperspectral indices could further improve accuracy of estimating severity of powdery mildew at early stages.

Each spectral region in hyperspectral images provides unique information about the plant. It is known that the visible and infrared regions of the electromagnetic spectra have close connection with the physiological stress levels in the plants (Muhammed, 2002, 2005; Xu *et al.*, 2007). Therefore, some of these wavebands can be used to detect plant diseases (West *et al.*, 2003), even before the symptoms are visible (Sankaran *et al.*, 2010). Therefore, 11 hyperspectral indices, reflecting physiological changes induced by plant diseases, were selected and used for discriminant and regression analysis of powdery mildew, together with PMI. Compared to the influence of individual PMI, to some extent, the addition of other indices improved detective accuracies of powdery mildew. The results of FDA implied that PMI had similar effect to the indices of PRI and ARI for classification of two disease levels,

but the combination of PRI, ARI and PSRI significantly increased identifying accuracies of leaves with low disease severities. Furthermore, the synthesis of PMI, PSRI and ARI can apparently decrease the estimating error of DI. For these results, it was easy to see that PMI was not chosen for a sensitive index in the three-class system. This could be related to various pigment changes in leaves early infected, such as chlorophyll, carotenoid and anthocyanin, which result in spectral variations in 530–570 nm spectral range. These wavelengths were included in indices of PRI and ARI, but not in PMI. The Photochemical Reflectance Index (PRI) could remotely assess photosynthetic efficiency at leaf scale, while Anthocyanin Reflectance Index (ARI) is closely related to anthocyanin content (Garbulsky *et al.*, 2011; Luo *et al.*, 2012).

Conclusion

This study found that early powdery mildew could result in observable spectral changes in both VIS/NIR regions, which make remote sensing detection of the early disease possible. Effective wavelengths or simple vegetation indices can be contributed to development of a portable or automated hyperspectral imaging device. Powdery mildew index (PMI) was constructed and showed significant capability of identifying diseased leaves from healthy leaves, although it had low classification accuracy for differentiating disease-damaged levels of early powdery mildew and low estimating accuracy for disease severity. However, accuracies of models improved with combination of other hyperspectral indices. It was indicated that the distinguishing model with the two indices of PRI and ARI has similar effect to that with PMI in two-class system of disease and health, but the model with the three indices of PRI, PSRI and ARI had significantly higher classification accuracy than that with PMI in three-class system of very slightly-damaged, slightly-damaged and healthy levels.

Acknowledgements

The study was supported by National Natural Science Foundation of China (Grant No. 41301505, 41771463, 41771469 and 41301471).

References

Behmann, J., J. Steinrücken and L. Plümer, 2014. Detection of early plant stress responses in hyperspectral images. *ISPRS J. Photogramm. Remote Sens*., 93: 98–111

Broge, N.H. and E. Leblanc, 2001. Comparing prediction power and stability of broadband and hyperspectral vegetation indices for estimation of green leaf area index and canopy chlorophyll density. *Remote Sens. Environ*., 2: 156–172

Cao, X., Y. Luo, Y. Zhou, X. Duan and D. Cheng, 2013. Detection of powdery mildew in two winter wheat cultivars using canopy hyperspectral reflectance. *Crop Prot.*, 45: 124–131

Chaerle, L. and D. Van der Staeten, 2000. Imaging techniques and the early detection of plant stress. *Trends Plant Sci*., 5: 495–501

Daughtry, C.S., C.L. Walthall, M.S. Kim, E.B. de Colstoun and J.E. McMurtrey, 2000. Estimating corn leaf chlorophyll concentration from leaf and canopy reflectance. *Remote Sens. Environ*., 2: 229–239

De Castro, A.I., R. Ehsani, R. Ploetz, J.H. Crane and J. Abdulridha, 2015. Optimum spectral and geometric parameters for early detection of laurel wilt disease in avocado. *Remote Sens. Environ*., 171: 33–44

de Jong, S.M., E.A. Addink, P. Hoogenboom and W. Nijland, 2012. The spectral response of buxus sempervirens to different types of environmental stress – a laboratory experiment. *ISPRS J. Photogramm. Remote Sens.*, 74: 56–65

Del Fiore, A., M. Reverberi, A. Ricelli, F. Pinzari, S. Serranti, A.A. Fabbri, G. Bonifazi and C. Fanelli, 2010. Early detection of toxigenic fungi on maize by hyperspectral imaging analysis. *Int. J. Food Microbiol*., 144: 64–71

Filella, I., L. Serrano, J. Serra and J. Penuelas, 1995. Evaluating wheat nitrogen status with canopy reflectance indices and discriminant analysis. *Crop Sci*., 5: 1400–1405

Gamon, J.A., J. Penuelas and C.B. Field, 1992. A narrow-waveband spectral index that tracks diurnal changes in photosynthetic efficiency. *Remote Sens. Environ*., 1: 35–44

Garbulsky, M.F., J. Peñuelas, J. Gamon, Y. Inoue and I. Filella, 2011. The photochemical reflectance index (PRI) and the remote sensing of leaf, canopy and ecosystem radiation use efficiencies: A review and meta-analysis. *Remote Sens. Environ*., 2: 281–297

Gitelson, A.A., M.N. Merzlyak and O.B. Chivkunova, 2001. Optical properties and nondestructive estimation of anthocyanin content in plant leaves. *Photochem. Photobiol*., 1: 38–45

Govender, M., K. Chetty and H. Bulcock, 2009. A review of hyperspectral remote sensing and its application in vegetation and water resource studies. *Water SA*, 2: 145–151

Haboudane, D., J.R. Miller, E. Pattery, P.J. Zarco-Tejad and I.B. Strachan, 2004. Hyperspectral vegetation indices and novel algorithms for predicting green LAI of crop canopies: Modeling and validation in the context of precision agriculture. *Remote Sens. Environ.*, 3: 337–352

Huang, L.S., D.Y. Zhang, D. Liang, L. Yuan, J.L. Zhao, G.S. Hu, S.Z. Du and X.G. Xu, 2013. Continuous wavelet analysis for diagnosing stress characteristics of leaf powdery mildew. *Int. J. Agric. Biol*., 15: 34–40

Huang, W., Q. Guan, J. Luo, J. Zhang, J. Zhao, D. Liang, L. Huang and D. Zhang, 2014. New optimized Spectral Indices for Identifying and Monitoring Winter Wheat Diseases. *IEEE J. Select. Trop. Appl. Earth Observ. Remote Sens.*, 7: 2516–2524

Jafari, M., S. Minaei, N. Safaie and F. Torkamani-Azar, 2016. Early detection and classification of powdery mildew-infected rose leaves using ANFIS based on extracted features of thermal images. *Infrar. Phys. Technol*., 76: 338–345

Kim, M.S., C.S.T. Daughtry, E.W. Chappelle and J.E. McMurtrey, 1994. The use of high spectral resolution bands for estimating absorbed photosynthetically active radiation (APAR). *Proc. 6th Int. Symposium on Physical Measurements and Signatures in Remote Sensing*, pp: 299–306. Val d'Isere, France

Kira, K. and L. Rendell, 1992. A practical approach to feature selection. *Proc. 9th Int. Workshop Mach. Learn., San Mateo, CA, USA*, pp: 249–256. Morgan Kaufmann Publishers Inc., Massachusetts, USA

Luo, J.H., W.J. Huang, L. Yuan, C.J. Zhao, S.Z. Du, J.C. Zhang and J.L. Zhao, 2012. Evaluation of spectral indices and continuous wavelet analysis to quantify aphid infestation in wheat. *Precis. Agric.*, 2: 151–161

Mahlein, A.K., T. Rumpf, P. Welke, H.W. Dehne, L. Plümer, U. Steiner and E.C. Oerke, 2013. Development of spectral indices for detecting and identifying plant diseases. *Remote Sens. Environ*., 128: 21–30

Mahlein, A.K., E.C. Oerke, U. Steiner and H.W. Dehne, 2012a. Recent advances in sensing plant diseases for precision crop protection. *Eur. J. Plant Pathol*., 133: 197–209

Mahlein, A.K., U. Steiner, C. Hillnhütter, H.W. Dehne and E.C. Oerke, 2012b. Hyperspectral imaging for small-scale analysis of symptoms caused by different sugar beet diseases. *Plant Methods*, 8: 3–15

Martinelli, F., R. Scalenghe, S. Davino, S. Panno, G. Scuderi, P. Ruisi, P. Villa, D. Stroppiana, M. Boschetti, L.R. Goulart, C.E. Davis and A.M. Dandekar, 2015. Advanced methods of plant disease detection. A review. *Agron. Sustain. Dev*., 1: 1–25

Merton, R. and J. Huntington, 1999. *Early Simulation of the ARIES-1 Satellite Sensor for Multi-temporal Vegetation Research Derived from AVIRIS*, pp: 299-307. Summaries of the Eight JPL Airborne Earth Science Workshop, Pasadena, JPL Publication, California, USA

Merzlyak, M.N., A.A. Gitelson, O.B. Chivkunova and V.Y. Rakitin, 1999. Non-destructive optical detection of pigment changes during leaf senescence and fruit ripening. *Physiol. Plant.*, 1: 135–141

Muhammed, H.H., 2005. Hyperspectral crop reflectance data for characterizing and estimating fungal disease severity in wheat. *Biosyst. Eng*., 1: 9–20

Muhammed, H.H., 2002. Using hyperspectral reflectance data for discrimination between healthy and diseased plants, and determination of damage-level in diseased plants. *In*: *IEEE: Proc. 31st Applied Imagery Pattern Recognition Workshop*, pp: 49–54

Pu, R., M. Kelly, Q. Chen and P. Gong, 2008. Spectroscopic determination of health levels of coast live oak (*Quercus agrifolia*) leaves. *Geocarto Int.*, 23: 3–20

Ray, M., A. Ray, S. Dash, A. Mishra, K.G. Achary, S. Nayak and S. Singh, 2017. Fungal disease detection in plants: Traditional assays, novel diagnostic techniques and biosensors. *Biosens. Bioelectron.*, 87: 708–723

Rumpf, T., A.K. Mahlein, U. Steiner, E.C. Oerke, H.W. Dehne and L. Plümer, 2010. Early detection and classification of plant diseases with Support Vector Machines based on hyperspectral reflectance. *Comput. Electron. Agric*., 1: 91–99

Robnik-Sikonja, M. and I. Kononenko, 2003. Theoretical and empirical analysis of ReliefF and RReliefF. *Mach. Learn*., 53: 23–69

Sankaran, S., A. Mishra, R. Ehsani and C. Davis, 2010. A review of advanced techniques for detecting plant diseases. *Comput. Electron. Agric*., 1: 1–13

Steiner, U., K. Buerling and E.C. Oerke, 2008. Sensor use in plant protection. *Gesunde Pfianzen*, 4: 131–141

Thenkabail, P.S., R.B. Smith and E. De Pauw, 2000. Hyperspectral vegetation indices and their relationships with agricultural crop characteristics. *Remote Sens. Environ*., 2: 158–182

West, J.S., C. Bravo, R. Oberti, D. Lemaire, D. Moshou and H.A. McCartney, 2003. The potential of optical canopy measurement for targeted control of field crop diseases. *Annu. Rev. Phytopathol*., 41: 593–614

Xu, H.R., Y.B. Ying, X.P. Fu and S.P. Zhu, 2007. Near-infrared spectroscopy in detecting leaf miner damage on tomato leaf. *Biosyst. Eng*.,96: 447–454

Yang, X., H. Hong, Z. You and F. Cheng, 2015. Spectral and image integrated analysis of hyperspectral data for waxy corn seed variety classification. *Sensors* (*Basel*), 7: 15578–15594

Yuan, L., Y. Huang, R.W. Loraamm, C. Nie, J. Wang and J. Zhang, 2014. Spectral analysis of winter wheat leaves for detection and differentiation of diseases and insects. *Field Crop. Res.*, 156: 199–207

Zhang, J.C., R.L. Pu, J.H. Wang, W.J. Huang, L. Yuan and J.H. Luo, 2012. Detecting powdery mildew of winter wheat using leaf level hyperspectral measurements. *Comput. Electron. Agric*., 85: 13–23

(Received 20 March 2018; Accepted 16 April 2018)